A frequency stabilization method for diode lasers utilizing low-field Faraday polarimetry

J. A. Kerckhoff, C. D. Bruzewicz, R. Uhl,[a)] and P. K. Majumder
Physics Department, Williams College, Williamstown, Massachusetts 01267

We present a method of diode laser frequency stabilization based on the Faraday rotation of linearly polarized light passing through an atomic sample in the presence of a very modest (1 mT) magnetic field. Near the zero crossing of this spectroscopic feature, an optical system capable of very precise polarimetry detects and corrects for very small frequency fluctuations via a feedback system, which keeps the rotation signal at zero. In our application, we have demonstrated robust frequency stabilization over time scales from 10 ms to 1 h at the 1 MHz level or below. We utilize this technique to lock our laser to a "forbidden" M1/E2 transition in thallium at 1283 nm, for which saturated absorption techniques are not straightforward. This technique has broad applicability to spectroscopy of various atomic systems as we also demonstrate using a Rb cell and a 780 nm diode laser. © *2005 American Institute of Physics.* [DOI: 10.1063/1.2038305]

INTRODUCTION

Many applications in high-precision spectroscopy take advantage of the convenience, affordability, and long lifetime of semiconductor diode lasers. Extended cavity geometries of several varieties can provide stable, tunable, single-longitudinal-mode operation from these devices. However, when spectroscopy requirements dictate frequency stability at or below the 1 MHz level over time scales of minutes or hours, additional stabilization measures are necessary. Common among these are the use of a second, stable, high-finesse optical cavity, and the use of saturated absorption or other Doppler-free atomic resonance techniques[1,2] to detect frequency drift through changes in the transmission of a supplementary atomic vapor cell. A rather different stabilization technique[3] compares transmission peaks of an "unknown diode" laser with a reference (stabilized) HeNe laser passing through a scanning Fabry-Perot optical cavity. While we have utilized this particular scheme in our laboratory, it is limited to very low feedback bandwidth (~30 Hz) and cannot reduce short-term (millisecond time scale) diode laser frequency jitter.

It has been demonstrated that magneto-optical techniques can provide an effective tool for diode laser frequency stabilization.[4,5] In one application, a large magnetic field (~100 mT) was used to induce a substantial Zeeman splitting in an atomic vapor cell of rubidium, leading to a differential absorption of circular polarization components of incident laser light. Although the sensitivity of the signal to frequency changes was not enhanced by Doppler narrowing in this case, the large capture range and high signal-to-noise ratio resulted in a robust sub-MHz frequency stabilization scheme.[4]

For our application, we have a tunable "Littrow" configuration extended cavity diode laser system near 1283 nm.

We require this laser to be locked near the frequency of a "forbidden" M1/E2 transition in atomic thallium. Saturation spectroscopy techniques, routine for the case of E1 transitions, would involve much greater technical challenges for our case of a low-power diode laser tuned to this much weaker transition. We have instead developed a new magneto-optic stabilization scheme that allows the use of low magnetic fields of order 1 mT, a factor of 100 smaller than that required for other schemes,[4,5] and generated by a solenoid rather than permanent magnets. Very sensitive polarimetry then provides a high signal-to-noise Faraday optical rotation signal (in contrast to the differential absorption signals utilized in Ref. 4). By feeding back from the rotation angle signal to the piezo control of the laser, we achieve robust stabilization of the laser frequency over time scales from 10 ms to several hours.

We use a quartz vapor cell of thallium and must use an oven to heat the cell to near 800 °C in order to achieve sufficient number density to detect the weak M1 transition that we study. Yet the technique we describe could, of course, be extended to other species, and to E1-allowed transitions, indeed, to situations in which such extreme cell heating would not be necessary. To demonstrate this broad applicability, we have also inserted a room-temperature rubidium cell into our polarimeter, and used a second diode laser tuned to the D1 line at 780 nm (see Sec. VI). We show that the quality of the rubidium polarimeter signal would allow frequency stabilization of equivalent precision for this laser system.

I. LOW-FIELD FARADAY ROTATION LINE SHAPE

The Faraday effect describes the optical rotation of linearly polarized light when passing through a medium with an applied magnetic field parallel to axis of laser propagation. The magnetic field, B, causes the Zeeman splitting of levels with different m_F with a frequency shift given by

---

[a)]Electronic mail: Ralph.Uhl@williams.edu

$$\delta\omega = g_F \frac{\mu_B B}{\hbar} m_F, \tag{1}$$

where μ_B is the Bohr magneton and g_F is the Landé g-factor. This has the effect of shifting the resonant frequencies for absorption of σ^+ and σ^- light tuned near to an atomic resonance at $\hbar\omega_{ij} = E_i - E_j$. In addition to this field-induced differential shift in absorption resonance frequency, there is an associated frequency-dependent difference between the real parts of the refractive index n of the two circular components of light. This leads to an optical rotation of light at frequency ω over an interaction length L, which can be expressed as

$$\Phi_F(\omega) = \frac{\omega L}{c} \Re\left[\frac{n_+(\omega) - n_-(\omega)}{2} \right]. \tag{2}$$

In the limit of small applied magnetic field, B, the associated change in the refractive index will be small, $n_\pm(\omega) \cong n(\omega \pm \delta\omega)$. The low-field Faraday rotation signal is thus proportional to

$$\Phi_F(\omega) \propto B \Re\left[\frac{\delta n}{\delta\omega} \right]. \tag{3}$$

The peak amplitude of the rotation scales with both applied field and with atomic number density, while the frequency dependence of the optical rotation signal takes the form of the derivative of the dispersion curve, a symmetric line shape with two zero crossings:

$$\Phi_F(\omega) \propto D'(\omega), \tag{4}$$

where

$$D'(\omega) = \frac{d}{d\omega}\left[\frac{\omega - \omega_{ij}}{(\omega - \omega_{ij})^2 + \gamma^2/4} \right] = \frac{\gamma^2/4 - (\omega - \omega_{ij})^2}{[(\omega - \omega_{ij})^2 + \gamma^2/4]^2}. \tag{5}$$

Here, γ is the homogeneous linewidth (in our case dominantly due to collisional broadening). While retaining this same basic shape, the details of the line shape become more complicated in larger magnetic fields as the Zeeman shift becomes significant compared to this linewidth. Indeed, there is a field strength for which the observed peak optical rotation maximizes. In practice, we operate in the vicinity of this limit, since in that case, the dependence of the rotation signal on magnetic field, and hence the sensitivity to field fluctuation and drifts, is much reduced. The overall width of our experimental line shapes are determined to a large degree by Doppler broadening. A complete line-shape analysis therefore requires the convolution of the homogeneous and inhomogeneous widths. Also, the presence of additional unresolved isotopic and hyperfine transitions complicate our line shape, as do small contributions to the observed optical rotation signal due to hyperfine state mixing in the magnetic field. Comprehensive line-shape analysis and precise fitting of these experimental signals, while undertaken for previous experiments,[6,7] are not required for the frequency stabilization application discussed here.
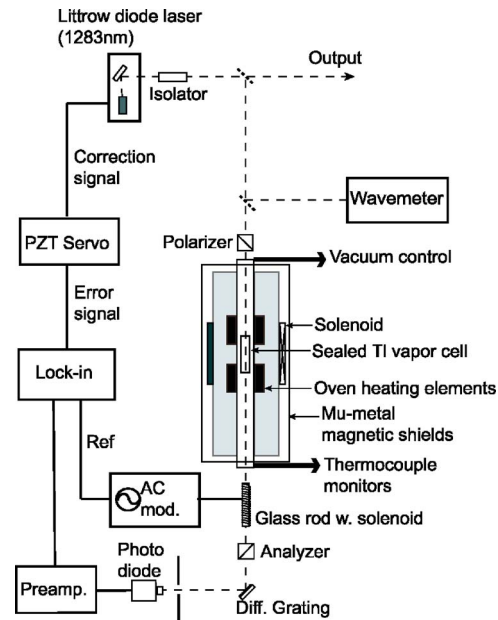

FIG. 1. Experimental setup showing the optical polarimeter, atomic vapor cell interaction region, and detection and feedback electronics.

II. EXPERIMENTAL DETAILS

A schematic drawing of the experimental setup is shown in Fig. 1. An external cavity diode laser (Sacher Lasertechnik, Model TEC 100) produces roughly 10 mW of 1283 nm light. A small amount of the light is directed to a wavemeter (Burleigh WA-1500) for a coarse wavelength measurement, and to a confocal Fabry-Perot cavity for frequency scan calibration.

Roughly 3 mW of laser light is directed into our polarimeter. It first passes through a calcite Glan-Thompson prism polarizer before it enters an evacuated ($\sim$100 Pa) 48-in. ceramic tube at the center of which is a 20-cm-long sealed quartz cell containing a few grams of atomic thallium. Surrounding the oven tube is a solenoid capable of producing a several mT magnetic field parallel to the direction of the light propagation. The central section of the ceramic tube that houses the cell is also surrounded by two pairs of external clamshell heaters, each driven by an alternating current of 4-5 A (rms) at $\sim$18 kHz supplied by four audio amplifiers (Gemini GXA-1600). Given the time constant of our detection signal, magnetic fields induced by the very-high-frequency AC heating currents contribute no detectable noise to our system. The magnetic shielding requirements of this stabilization method are quite modest, although for other experimental work in our laboratory, we do employ a set of nested cylindrical mumetal magnetic shields with endcaps that offer roughly a 100-fold shielding factor for longitudinal fields (and a much larger factor for transverse fields).

In order to achieve the large number density required to detect the M1 transition that we study, cell operating temperatures are between 790 and 820 °C, at which we observe an M1 absorption of order 10%. At these temperatures, it is essential to surround the cell with an evacuated environment to prevent noise induced by convection currents of hot air near the cell. After passing out of our evacuated oven tube, a

second calcite prism is used as a polarization analyzer. Our detection system consists of an InGaAs photodiode plus low-noise preamplifier (Stanford Research Systems, SR560). The continuum infrared blackbody light of our hot oven, which is transmitted through the analyzer prism in abundance, is effectively filtered out by the use of a diffraction grating and collimator upstream of the detector.

It is important to optimize the extinction factor of the polarimeter to minimize noise from background laser transmission through the system. While our calcite prisms transmit only 10^{-7} of the incident light when used in isolation, the cell and other optical surfaces between the polarizers in practice limits this "finite extinction" to 10^{-5}. We can model this phenomenon as due to an effective uncrossing angle, ϕ_0, where $\phi_0^2 = 10^{-5}$. In practice, this produces a signal-to-background ratio of about 1, since the atomic Faraday rotation amplitudes are of the same order as ϕ_0. In order to facilitate manual polarization control with the required precision, we mount our polarizers on a mechanical lever arm whose position is determined by the position of a dual micrometer head. In this way we can reliably control and calibrate the rotation of our polarizers to better than 10 μrad. We emphasize that for our application, much of the engineering has gone into the creation of the heated cell/evacuated oven tube assembly. For more "conventional" applications of this technique to room-temperature vapor cells, the overall setup would be substantially simpler and more compact.

III. SIGNAL PROCESSING AND POLARIZATION ANALYSIS

Referring again to Fig. 1, the key feature of our polarimeter is a 10-cm-long glass rod possessing a high Verdet constant (Hoya, FR-5 glass) that is positioned just before our analyzer prism. We apply an AC current of roughly 2 A (rms) at frequency $\omega_m/2\pi = 1200$ Hz to a small solenoid surrounding this rod, causing a sinusoidal modulation of the polarization of amplitude several mrad. This technique[6–8] has been used effectively to resolve optical rotations down to the μrad level in parity nonconservation experiments. Because the overall optical rotation remains in the small-angle limit, the transmitted intensity through the second, crossed polarizer can be expressed as

$$I(t) = I(\nu)\sin^2[\Phi_m \sin(\omega_m t) + \Phi_F(\nu)]$$
$$\approx I(\nu)[\Phi_m \sin(\omega_m t) + \Phi_F(\nu)]^2$$
$$\approx I(\nu)[1/2\Phi_m^2 + \Phi_F^2(\nu) - 1/2\Phi_m^2 \cos(2\omega_m t)$$
$$+ 2\Phi_m\Phi_F(\nu)\sin(\omega_m t)], \tag{6}$$

where Φ_m is the rotation amplitude of the modulator and $\Phi_F(\nu)$ is the Faraday rotation signal produced by the vapor cell. For simplicity here we have left out the DC term accounting for the finite extinction of the polarizers. When the calcite polarizers are crossed, and the atomic sample causes no Faraday rotation, the transmitted intensity of the polarimeter exhibits modulation at frequency $2\omega_m$ only. The system is linearly sensitive to small atomic Faraday rotations through detection of the intensity component at the first harmonic frequency ($1\omega_m$), which we extract via a digital
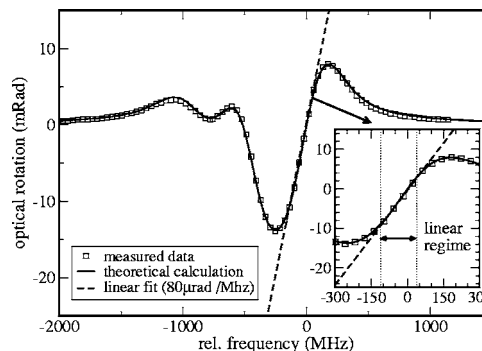

FIG. 2. Measured and theoretical Faraday rotation line shapes. This scan was completed in 30 s using a magnetic field of roughly 1 mT. The theory curve (solid line) accounts for the transmission envelope, all hyperfine and isotopic substructures, as well as a small dispersive line-shape contribution from magnetic-field-induced state mixing. The insert shows the linear portion of the line shape that we use to provide feedback to lock our laser.

lock-in amplifier (Stanford Research Systems SR810). Using a lock-in amplifier to detect the rotation signal has the additional advantage of eliminating sensitivity to a number of sources of low-frequency noise. We note that a second lock-in detecting the $2\omega_m$ component of the transmitted signal is insensitive to atomic rotation, and becomes an ideal monitor of the overall transmission (i.e., absorption) signal, $I(\nu)$.

As can be seen from Eq. (6), the $1\omega_m$ component of the transmitted light actually represents the *product* of the rotation and transmission signals of the atomic sample. In our case, with fairly modest overall absorption, this simply reduces the measured peak amplitude of the rotation signal by a small factor. Since the rotation signal itself scales linearly with number density, in this density regime there is a fairly weak dependence of peak lock-in signal with temperature. Figure 2 shows a typical Faraday rotation signal taken for the thallium $6P_{1/2} \rightarrow 6P_{3/2}(F = 1 \rightarrow F' = 1, 2)$ M1/E2 transition for a cell temperature of 800 °C. One can see that the theoretical model we have developed agrees very well with the data. We note that the linear region on the high-frequency side of this curve, extending over nearly 200 MHz, allows a wide range of potential lock points in our stabilization scheme. The slope of this feature is 80 μrad/MHz, and (as mentioned) various only slightly in this temperature/atomic density regime (a few percent over ±20 °C). Since our peak Faraday rotation signal is only 10 mrad, the very high signal-to-noise ratio (evident in the 30-s scan shown here) is essential for precise angle resolution and eventual frequency stabilization. To quantify the residual polarization fluctuations in our system, we simply sample the lock-in output signal for some time, and then, using our calibrated mechanical lever, "uncross" one polarizer by a known amount. Figure 3 shows the result of this experiment, taken in the absence of a magnetic field (hence without any Faraday rotation signal). We measure a baseline rms noise of 8 μrad over this 10-s period. The effective frequency bandwidth for these data is determined by the lock-in time constant (1 ms) and filter rolloff (18 dB/oct) to be ~160 Hz. With the magnetic field turned on, and the laser tuned near the zero crossing of the Faraday rotation line shape, we observe increased rotation noise as a
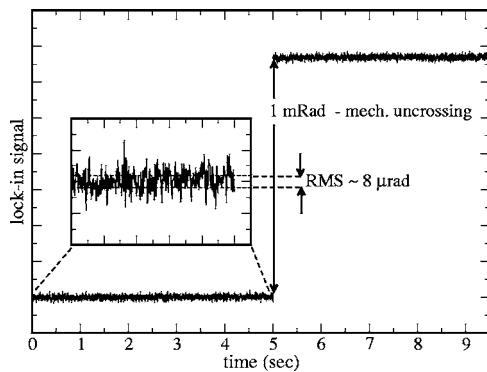
FIG. 3. Lock-In signal angle calibration is achieved by applying a known mechanical uncrossing of the analyzer. There is no atomic Faraday signal here, and the lock-in time constant was 1 ms.

result of laser frequency fluctuations. We can interpret rotation noise measurements in terms of effective frequency noise using the line-shape slope from Fig. 2. Our 8 μrad angle noise measurement thus sets a lower limit of 0.1 MHz to the size of frequency fluctuations to which we are potentially sensitive.

IV. FREQUENCY STABILIZATION RESULTS

In preparation for laser locking, we tune our diode laser near to the zero-crossing point on our Faraday rotation line shape. Our goal is then to steer the system back to zero rotation by feedback to the piezoelectric transducer (PZT) controlling the diode laser frequency. A standard servo circuit (see, for example, Ref. 1) monitors the rotation angle signal via the lock-in output and produces a correction signal that is suitably amplified and sent to the laser PZT control. By setting the servo circuit time constant to be short (<0.1 ms), the effective bandwidth of the entire feedback loop is then determined by the easily adjusted time constant and filter parameters of the lock-in amplifier. Figure 4 shows three comparative 10-s scans of the lock-in output signal. On top is the free-running optical rotation signal taken under the
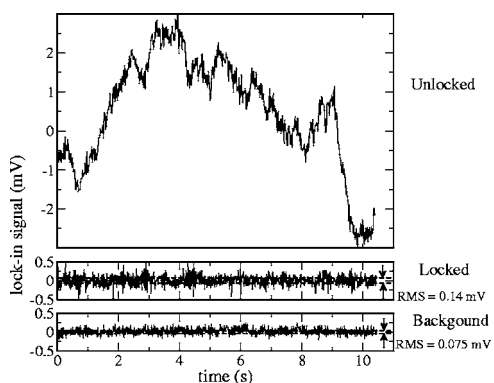

FIG. 4. Near the Faraday rotation zero crossing, the lock-in output shows substantial fluctuations due to laser frequency noise (top trace). In servo mode (middle trace), we observe a roughly 20-fold reduction in these fluctuations. Residual fluctuations are roughly two times the size of the intrinsic polarimeter noise (bottom trace). Given the angle calibration (Fig. 3) and the line-shape slope (Fig. 2), the servo-mode noise corresponds to a residual frequency fluctuation of 0.28 MHz (rms), with an equivalent noise bandwidth of 160 Hz.
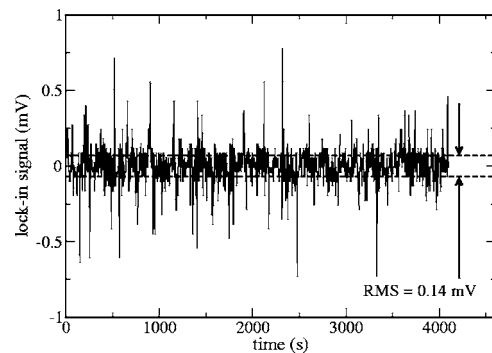

FIG. 5. Longer-term behavior of the system in servo mode shows no additional noise beyond that shown in Fig. 4.

same operating conditions as in Fig. 2 with the laser tuned near the Faraday rotation zero-crossing point. Below this is the rotation signal in servo mode, showing a suppression of noise of more than an order of magnitude. The bottom trace indicates that we are within a factor of two of the intrinsic polarimeter noise while operating in the servo mode. We calibrate the voltage signal in terms of optical rotation (in μrad) by the mechanical uncrossing of the analyzer prism discussed above, and convert to effective frequency using the known line-shape slope (Fig. 2). Thus, the error signal shown in Fig. 4 corresponds to an rms frequency noise of 0.28 MHz (160 Hz bandwidth). It is important to note that we have not compared the frequency stability of our locked laser to any reference laser. Thus, we cannot rule out the possibility that some source of frequency noise outside of the bandwidth of our servo system exists in our system, leading to poorer frequency stability than our error signal would imply. As can be seen, the unlocked diode laser exhibits two distinct regimes of frequency instability. Characteristic of these diode laser systems, there is both a slow ($\sim 1-10$ s) frequency drift with a magnitude of order 10 MHz and a much faster ($10-100$ ms time scale) frequency "jitter." Our servo loop eliminates the long-term drift and provides some reduction in the amplitude of the jitter.

To demonstrate the robustness of the stabilization method over longer time scales, we locked the laser for a period of several hours. A portion of the sampled lock-in output signal from such a run is shown in Fig. 5. No loss of lock or degradation in stabilization precision was observed in a number of trials of this duration.

In the above discussion we have locked our laser to the zero-crossing point of the Faraday rotation curve, however, a convenient feature of this scheme is the ability to tune the laser by simply applying a small DC current to our glass polarization modulation rod, while the system is in servo mode. This current has the same effect as a small uncrossing of the polarizers. The servo system will then steer back to the zero rotation condition, except that the new frequency lock point would be located away from the true zero crossing of the Faraday rotation curve. This tuning method offers a nearly 200-MHz range, as can be seen in Fig. 2. For our long-term experimental goal, we must tune the laser to the side of the resonance line, making the zero-crossing point of the Faraday rotation line shape an ideal lock point. For other

applications a straightforward use of an acousto-optic modulator to shift the frequency of laser light sent to the polarimeter would allow one to lock near the center of an atomic transition.

V. POTENTIAL SYSTEMATIC ERRORS AND ACCURACY LIMITATIONS

To assess the viability of this stabilization method, it is not sufficient to merely demonstrate the noise reduction discussed above. It is important to consider a variety of potential sources of systematic error that could affect the long-term accuracy of the frequency lock. As this method relies on a low-field magneto-optic effect, principle among these is the influence of stray magnetic fields and field fluctuations. Magnetic field changes affect the Faraday rotation line shape in two ways. First, the overall amplitude of the line shape scales with the field. This dependence is linear only in the "small-field" limit, and becomes much weaker at larger fields, a useful feature that we exploit. If our frequency servo system is operated as demonstrated here, locking to the true zero crossing of the Faraday rotation curve, there should be very little lock-point sensitivity to field fluctuations. Such a conclusion would then imply that this scheme could be used even in the absence of magnetic shielding. If one uses the tuning method described above to lock away from the true Faraday rotation zero-crossing point, fluctuations and drifts in the overall magnetic field would now influence the locking characteristics to some degree. Considering the data shown in Fig. 2, we observe a roughly 1000:1 signal-to-noise ratio for our optical rotation curves, with the 1-ms time constant of our lock-in. We typically use 1-mT fields in this work, and at this field strength, the scaling of Faraday rotation amplitude with field is quite weak. Given the measured dependence that we see, we can calculate that magnetic field fluctuations at or below the 5μT level (roughly 1/10 of typical ambient magnetic fields) would not measurably degrade the precision of our frequency lock over the entire linear capture range indicated in Fig. 2. Thus, this particular frequency tuning technique would become feasible with rather modest magnetic shielding of ambient fields. On the other hand, keeping the lock point at true Faraday rotation zero crossing (and then tuning the laser via any number of other methods) leaves us particularly insensitive to lock-point fluctuations arising from field-induced signal amplitude changes.

A second, less obvious sensitivity of our scheme to magnetic field variations comes through the dependence of the linewidth of the Faraday rotation curve to Zeeman splitting. Since the optical activity depends on the difference between two Zeeman-shifted dispersion curves, the exact line shape, and hence the zero-crossing point, will depend somewhat on the Zeeman splitting itself. In principle, such variation in zero-crossing frequency will translate directly into a change in laser frequency when in servo mode. In practice, we must also account for the (magnetic-field-independent) Doppler width of our line shapes, which is roughly ten times larger than the homogeneous widths, and thus dominates the observed experimental linewidths. The g-factors of the relevant thallium levels lead to a Zeeman shift slope of roughly 50 MHz/mT for our transition. We have generated simulated experimental line shapes by convolving the appropriate dispersion-difference curve with Gaussian Doppler profiles and have mapped out the exact dependence of the zero-crossing frequency on Zeeman splitting, which, in the vicinity of the typical fields used here, results in a roughly 20 MHz/mT zero-crossing dependence of the Faraday line shape on magnetic field. Given the current precision of our system, magnetic field fluctuations at or below the level of 0.01 mT (or roughly 1/5 of typical ambient magnetic fields) would not lead to a detectable loss of accuracy. Thus, the required control over the external magnetic field environment should not be prohibitive.

We note that none of the above conditions put a particularly stringent requirement on the quality of the current supply used for the Faraday solenoid. Nor is the homogeneity of the longitudinal field an issue, as the optical rotation simply depends on the integrated longitudinal field through the cell. Finally, it should be mentioned that magneto-optic effects due to transverse magnetic fields are sufficiently weak in comparison to the longitudinal-field Faraday effect discussed here that they are safely ignored.

Fluctuations in cell temperature could also be of concern, principally through the effect that this would have on the Doppler width of the transition. Such drifts would systematically change the zero-crossing point of our Faraday rotation curve, exactly as discussed above. In our case the large thermal mass and substantial insulation of our oven tends to keep the cell temperature stable at the 1 °C level once thermal equilibrium is reached (even without active temperature stabilization). It is easy to show that thermal variation at this level would lead to effective shifts in the lock frequency of order 0.1 MHz. While this is not significant at the current level of precision, it would be straightforward to reduce temperature variations by at least one order of magnitude by using an active stabilization method. Temperature variations also lead to changes in thallium vapor pressure and number density, and could potentially affect the line shape through changes in collisional broadening or shifts. Given previously measured temperature dependence of collisional widths in thallium vapor,[9] and given our level of temperature control, we are confident that such systematics lie well below our current experimental sensitivity.

A final concern to be discussed is the long-term mechanical stability of our polarimeter. Independent of the atomic sample, it is possible that over a time scale of hours, the rotation angle will drift due to slow mechanical "uncrossing" of the polarizers. If left uncorrected, this would obviously directly result in a laser frequency drift while the polarimeter is in the servo mode. In practice, this drift could be easily monitored by simply turning off the solenoid field and correcting any background polarization drift. To investigate whether this background drift was likely to be a significant limitation, we simply sampled the lock-in signal with no magnetic field present over the course of several hours. The lock-in time constant was set to be 100 ms, since we were only interested in very slow polarization variations. Figure 6 shows the results of this study. The long-term $\sim 1 \mu$rad stability of our polarimeter corresponds to an effective frequency drift of order 0.01 MHz. Clearly this system-
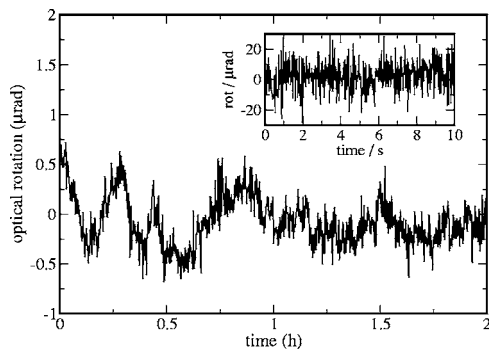
FIG. 6. Limits on the mechanical drift of the polarimeter in the absence of any atomic Faraday effect.

atic effect is not a concern for frequency stabilization at the 0.3 MHz level. The insert in this figure reinforces the point that this drift is nearly an order of magnitude less than the observed short-term polarimeter noise. In the first few minutes after adjusting optical elements, we tend to see somewhat larger polarimeter drifts, although still not large enough to be of concern.

VI. FARADAY POLARIMETRY USING A Rb CELL

To demonstrate the feasibility of our technique in a simpler and more conventional application, we have replaced our diode laser with another from the same supplier, in this case tuned to the 780 nm D1 transition in rubidium. A room-temperature Rb cell was inserted in place of our heated quartz thallium cell.

Although our optical system (antireflection coatings, grating efficiency, etc.) was not optimized for this wavelength, we were able to obtain high-quality Faraday rotation scans in comparable magnetic fields. Unlike the M1 transition we have discussed above, the ~3 mW of laser power used in our thallium experiment would induce substantial optical saturation for the case of this strongly allowed E1 transition in rubidium. Reducing the incident power to the point where such saturation effects are not significant makes us more susceptible to shot-noise limitations (recalling that we always work with nearly crossed polarizers). For this Rb work, we used a low-noise, small-area Si photodiode in conjunction with a high-gain preamplifier constructed from discrete components.[10] A productive approach, not pursued here, would be to expand the laser beam passing through the cell and refocus near the detector, reducing the susceptibility to optical saturation. With increased homogeneous linewidth (due to the natural width of this Rb transition), we note that a somewhat larger magnetic field can be used to increase the amplitude of the Faraday rotation curve in the case of Rb. A composite Faraday rotation curve in the vicinity of the Rb
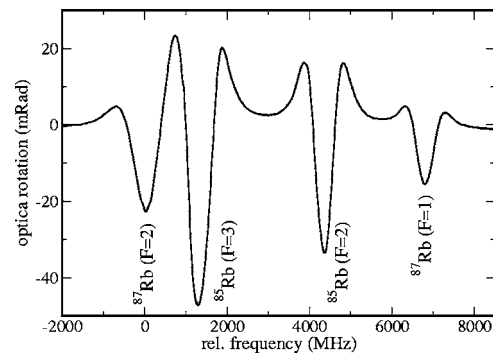

FIG. 7. Experimental Faraday rotation curve in the vicinity of the Rb D1 lines. This scan was taken with a 2.5-mT field, and required roughly 1 min to acquire. The lock-in time constant was set, as in the thallium work, to be 1 ms.

D1 lines is shown in Fig. 7. This scan was taken with a 2.5-mT magnetic field, and roughly 4 μW of laser power incident on the cell. The typical value of the steep slopes at the zero crossings of the various rotation line shapes shown in Fig. 7 are between 100 and 200 μrad/MHz, i.e., slightly larger than the thallium curves from Fig. 2 above. The free-running rms polarimeter noise under these reduced-light optical conditions corresponded to 20 μrad (using the identical detection bandwidth to that discussed above). This then implies an effective frequency noise baseline of 0.1–0.2 MHz. These measurements certainly indicate that frequency stabilization of this laser at the sub-MHz level using a room-temperature Rb cell should be straightforward using the low-field Faraday polarimetry technique described in this paper.

[1] K. B. MacAdam, A. Steinbach, and C. Wieman Am. J. Phys. **60**, 1098 (1992).
[2] Y. Yoshikawa, T. Umeki, T. Mukae, Y. Torii, and T. Kuga, Appl. Opt. **42**, 6645 (2003).
[3] W. Z. Zhao, J. E. Simsarian, L. A. Orozco, and G. D. Sprousea, , Rev. Sci. Instrum. **69**, 3737 (1998).
[4] K. L. Corwin, Z.-T. Lu, C. F. Hand, R. J. Epstein, and C. E. Wieman, Appl. Opt. **37**, 3295 (1998).
[5] V. V. Yashchuk, D. Budker, and J. R. Davis, Rev. Sci. Instrum. **71**, 341 (2000).
[6] P. K. Majumder and L. L. Tsai, Phys. Rev. A **60**, 267 (1999).
[7] P. A. Vetter, D. M. Meekhof, P. K. Majumder, S. K. Lamoreaux, and E. N. Fortson, Phys. Rev. Lett. **74**, 2658 (1995).
[8] D. M. Meekhof, P. A. Vetter, P. K. Majumder, S. K. Lamoreaux, and E. N. Fortson, Phys. Rev. A **52**, 1895 (1995).
[9] P. A. Vetter, Ph.D. thesis, University of Washington 1995.
[10] S. R. Jefferts and F. L. Walls, Rev. Sci. Instrum. **60**, 1194 (1989).